Sensor fault detection and isolation using a support vector machine for vehicle suspension systems

Kicheol Jeong, Seibum B. Choi, *Member, IEEE* and Hyungjeen Choi

***Abstract*—In this paper, a means of generating residuals based on a fault isolation observer (FIO) and evaluating them using a support vector machine (SVM) is proposed. The proposed FIO generates the isolated residual signals and they shows robust performance regardless of unknown road surface conditions. This FIO is designed using a linear time-invariant quarter-car model. While quarter-car models have the form of a bilinear system, in this study the authors convert this bilinear model to a linear model with model uncertainty based on the assumption that the control input is limited. Therefore, the proposed FIO can be used regardless of the type of damper or controller. Furthermore, the SVM based residual evaluator without empirically set thresholds is used to evaluate the generated residuals. The proposed fault diagnosis algorithm is expected to reduce the effort required in the design procedure and it can also detect a small amount of sensor fault that cannot be detected by traditional limit-checking method. The proposed fault diagnosis algorithm is verified using low cost production accelerometers and a quarter-car test rig. Consequently, the fault diagnosis algorithm proposed in this paper can detect the faults of a sprung mass accelerometer and an unsprung mass accelerometer independently, and this algorithm can reduce the effort required in designing the diagnosis algorithm greatly.**

***Index Terms*—fault detection and isolation, support vector machine, eigenstructure assignment, vehicle suspension, sensor fault diagnosis**

I. INTRODUCTION

THE suspension system of modern vehicles is an essential component to guarantee the ride quality, stability and handling performance of the vehicle. In terms of the control method, the vehicle suspension system can be classified as passive, semi-active, or active suspension. The passive suspension, which does not utilize any control input, is generally used in the automotive industry. However, this type of suspension cannot satisfy the desired ride quality and handling performance since these two characteristics have a trade-off relationship. To overcome this limitation, semi-active and active suspension systems are increasingly used in the automotive industry. Active suspension achieves control objectives using an additional actuator such as a motor. Although this type of suspension can provide high performance, it is not widely used due to excessive energy consumption, load increase, and packaging issues. In contrast, majority of automotive manufacturers adopt semi-active suspensions that adjust the damping characteristics of the suspension to solve packaging and energy issues. Since the semi-active suspension is widely adopted in the automotive industry, many researchers have conducted studies to enhance the performance of semi-active suspension systems [1]–[10].

These control algorithms improve the ride quality and stability of the vehicle. However, if a fault occurs on the control system components, it impacts vehicle performance and stability negatively. In particular, since the vehicle suspension control system consists of many sensors and actuators, there is a high probability that the system will collapse due to faults. Therefore, in order to improve the performance and stability of the vehicle, a fault diagnosis algorithm as well as a control algorithm is required. In recent years, the electronization of automobiles is a trend in the global automobile industry, and various sensors are embedded in the vehicle. For this reason, all vehicle manufacturers have implemented fault diagnosis algorithms for vehicle sensor systems.

Today, most automotive manufacturers adopt the limit-checking method [11] which determines sensor faults based on predetermined sensor signal thresholds. However, this method has poor fault detection performance since the sensor signal threshold is set high to ensure robustness of the fault diagnosis algorithm.

Therefore, a model-based fault diagnosis method [11]–[16] using a physical model of a system has recently been studied to design a robust and sensitive fault diagnosis algorithm. A model-based fault diagnosis algorithm consists of a residual generator that generates a fault-sensitive residual and a residual evaluator that evaluates the residual signal.

Recently, model-based fault diagnosis algorithms for automotive suspension systems have been extensively studied. In particular, many studies have been conducted using a quarter-car model which is mainly used for the design of a suspension control algorithm. In general, quarter car suspension system includes both the nonlinear characteristics of the damper and unknown road input. Therefore, when designing a suspension fault diagnosis algorithm, it is important to ensure robustness against unknown road input and nonlinearity of the damper. Recently, various methods have been proposed to achieve these design objectives. Chamseddine [17] used a quarter-car model based sliding mode observer to diagnose sensor faults in the vehicle suspension system. Although the fault diagnosis algorithm is robust to disturbance, an additional sensor such as a displacement sensor is used instead of the sensor configuration commonly used in commercial vehicles [18]. Bornor [19] and Varrier [20] used the parity space approach, a well-known model-based fault diagnosis method. However, the residual generator constructed by the parity space approach cannot guarantee robustness against modeling

K. Jeong and S. B. Choi are with the Korea Advanced Institute of Science and Technology, Daejeon 34141, South Korea (e-mail: cbrxxiq@kaist.ac.kr; sbchoi@kaist.ac.kr). H. Choi is with the Korea Automotive Technology Institute, 303 Pungse-ro, Pungse-myeon, Dongnam-gu, Cheonan-si, Chungnam 31214, South Korea (e-mail: hjchoi@katech.re.kr).

uncertainties. Alternatively, Kim [21] proposed a method of diagnosing a sprung mass accelerometer based on a full-car model, this method cannot diagnose a fault of unsprung mass accelerometer and it is difficult to find roll dynamics properties used in this paper.

In model-based fault diagnosis schemes, the residuals generated by a fault detection algorithm are not zero because of model uncertainties, disturbances, and sensor noise that are not considered. Therefore, the design of rational residual evaluation algorithm is essential to the design of fault diagnosis algorithm. However, in most of the previous studies, residual evaluation is performed using a fixed threshold defined empirically. Although Kim [21] proposed an adaptive threshold method, the form of the adaptive threshold was also determined empirically. In addition, little research has been carried out to diagnose fault of vehicle suspension system using the sensor configuration of most vehicle produced today.

In order to overcome these limitations, this paper proposes a robust quarter-car model based suspension sensor fault diagnosis algorithm for unknown road input and damping coefficient changes. The quarter-car model of the semi-active suspension is represented as a bilinear system [22] in which there is coupling of the unmeasured state and the control input. In this paper, this bilinear model is converted into a linear model with unknown parametric uncertainty to design a fault detection and isolation (FDI) algorithm using the eigenstructure assignment method. The proposed FDI algorithm can generate residuals using only the sensors built into the vehicle, regardless of the type of controller or damper. In addition, this paper also uses the support vector machine (SVM) [23]–[26], a widely used machine learning technique, to evaluate residual signals. In this paper, the feature required for the SVM learning process is created by model-based fault diagnosis technique. This method allows an accurate residual evaluation while reducing the effort for threshold tuning to evaluate residuals.

This paper is organized as follows. In section II, faults in the sprung mass accelerometer and the unsprung mass accelerometer are represented by a state space linear model. In this section, sensor faults are converted to pseudo-actuator faults. In section III, FDI algorithm consisting of a fault isolation observer (FIO) based residual generator and SVM based residual evaluator is presented. The eigenvalues of the proposed FIO are assigned considering the performance index of the fault diagnosis algorithm in a specific frequency region. In addition, the residuals generated by FIO based residual generator are evaluated using SVM. Section IV presents experimental verification using a quarter car test rig. In conclusion, this paper shows that the proposed FDI algorithm provides robust performance under various road inputs.

II. Modeling faults of the vehicle suspension

In this section, faults in the sprung mass accelerometer and unsprung mass accelerometer are demonstrated by the quarter-car model. To apply the eigenstructure assignment method, which is a linear fault diagnosis technique, this bilinear system is transformed into a linear system containing bounded model uncertainty. This conversion is performed under the reasonable assumption that the damping coefficient is limited. In addition, in order to design a diagnostic observer, faults in a sprung mass accelerometer and an unsprung mass accelerometer are transformed into a pseudo-actuator faults.

TABLE I
Quarter-car model properties

Symbol	Quantity	Value
m_s	Sprung mass	374.03 kg
m_u	Unsprung mass	52.25 kg
k_s	Spring coefficient	22080 N/m
k_t	Tire vertical stiffness	248193 N/m
c_n	Damper nominal damping coefficient	1562 Ns/m
c_u	Control input	$0 \leq c_u \leq 6096.77$ N/m

A. Quarter-car suspension model

A quarter-car suspension model has been widely used for suspension control studies due to the simplicity and accuracy of the model. The governing equations of a quarter-car suspension model such as that in Fig. 1 are as follows:

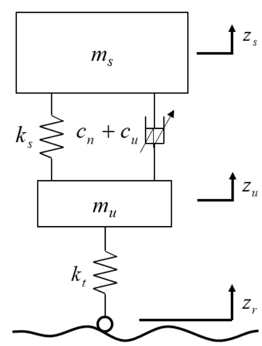

Fig. 1. Quarter-car model of a vehicle suspension.

$$m_s\ddot{z}_s = -k_s(z_s - z_u) - (c_n + c_u)(\dot{z}_s - \dot{z}_u) \tag{1}$$

$$m_u\ddot{z}_u = -k_s(z_u - z_r) - (c_n + c_u)(\dot{z}_u - \dot{z}_r) - k_t(z_u - z_r) \tag{2}$$

where m_s is a sprung mass, m_u is an unsprung mass, k_s is a spring coefficient, c_n is a nominal damping coefficient, c_u is a control input, z_s and z_u are displacement of sprung mass and unsprung mass and z_r is the road displacement. As in previous studies, the damping effect of tires is neglected. Table I lists the quarter-car model properties.

This governing equations can be expressed as a bilinear system. The state-space representation of this system is given as

$$\begin{aligned} \dot{x} &= \tilde{A}x + A_u x \cdot c_u + E_r \dot{z}_r \\ y &= \tilde{C}x + C_u x \cdot c_u \end{aligned} \tag{3}$$

where $x = \begin{bmatrix} z_s - z_u & \dot{z}_s & z_u - z_r & \dot{z}_u \end{bmatrix}^T$,

$$\tilde{A} = \begin{bmatrix} 0 & 1 & 0 & -1 \\ -k_s/m_s & -c_n/m_s & 0 & c_n/m_s \\ 0 & 0 & 0 & 1 \\ k_s/m_u & c_n/m_u & -k_t/m_u & -c_n/m_u \end{bmatrix},$$

$A_u = \begin{bmatrix} 0 & 0 & 0 & 0 \\ 0 & -1/m_s & 0 & 1/m_s \\ 0 & 0 & 0 & 1 \\ 0 & 1/m_u & 0 & -1/m_u \end{bmatrix}$, $y = \begin{bmatrix} \ddot{z}_s & \ddot{z}_u \end{bmatrix}^T$,
$\tilde{C} = \begin{bmatrix} -k_s/m_s & -c_n/m_s & 0 & c_n/m_s \\ k_s/m_u & c_n/m_u & -k_t/m_u & -c_n/m_u \end{bmatrix}$,
$C_u = \begin{bmatrix} 0 & -1/m_s & 0 & 1/m_s \\ 0 & 1/m_u & 0 & -1/m_u \end{bmatrix}$
and $E_r = \begin{bmatrix} 0 & 0 & -1 & 0 \end{bmatrix}^T$.
In the real world, the nominal damping coefficient c_n of a vehicle suspension has high nonlinear and hysteresis characteristics. In addition, according to (3), the control input is combined with a state variable, which is unknown. Furthermore, the damping control command and the actual damping control input are not the same due to physical limitations such as the actuator bandwidth. These system characteristics make designing fault diagnosis algorithms and analyzing fault diagnosis performance difficult. Although bilinear fault diagnosis algorithms have been studied [27], it is difficult to obtain robustness against damping coefficient uncertainty in such fault diagnosis algorithms. Therefore, in this paper, this bilinear system is transformed into a linear system with bounded parametric uncertainty. This transformation is based on a reasonable assumption that the damping coefficient of vehicle suspension is limited. According to Table I, the overall damping coefficient c_u+c_n is bounded between c_{max} (1562.00 Ns/m) and c_{min} (7658.77 Ns/m). Consequently, the bilinear system (3) can be represented as

$$\begin{aligned} \dot{x} &= Ax + E_u d + E_r \dot{z}_r \\ y &= Cx + F_u d \end{aligned} \tag{4}$$

where $A = \begin{bmatrix} 0 & 1 & 0 & -1 \\ -k_s/m_s & -c_0/m_s & 0 & c_0/m_s \\ 0 & 0 & 0 & 1 \\ k_s/m_u & c_0/m_u & -k_t/m_u & -c_0/m_u \end{bmatrix}$,
$C = \begin{bmatrix} -k_s/m_s & -c_0/m_s & 0 & c_0/m_s \\ k_s/m_u & c_0/m_u & -k_t/m_u & -c_0/m_u \end{bmatrix}$,
$E_u = \begin{bmatrix} 0 & -c_d/m_s & 0 & c_d/m_u \end{bmatrix}^T$,
$F_u = \begin{bmatrix} -c_d/m_s & c_d/m_u \end{bmatrix}^T$, $d = \Delta G x$, $|\Delta| \leq 1$,
$G = \begin{bmatrix} 0 & 1 & 0 & -1 \end{bmatrix}$.
where $c_0 = (c_{max} + c_{min})/2$ and $c_d = (c_{max} - c_{min})/2$.
Note that this linear system has bounded uncertainty since Δ and system state x are bounded. Consequently, it is possible to apply linear fault diagnosis techniques to the transformed system. It is noteworthy that this converted model can be used regardless of the type of damper controller and the hysteresis characteristics of the damper. The proposed linear model can be obtained under the assumption that c_{max} and c_{min} are known variables.

B. Pseudo-actuator fault modeling

According to the quarter-car model obtained in the above subsection, the fault model of the vehicle suspension can be represented as

$$\begin{aligned} \dot{x} &= Ax + E_u d + E_r \dot{z}_r + \tilde{E}_f \tilde{f} \\ y &= Cx + F_u d + \tilde{F}_f \tilde{f} \end{aligned} \tag{5}$$

where $\tilde{f} = \begin{bmatrix} f_s & f_u \end{bmatrix}^T$, f_s is the fault of the sprung mass accelerometer and f_u is the fault of the unsprung mass accelerometer.
Note that $\tilde{f}$ is an unknown fault vector that represents all possible types of sensor faults and should be zero on a healthy system. It is assumed that $\tilde{E}_f$ is zero, since the actuator faults are not considered in this paper. In (5), $\tilde{F}_f$ is modelled by an identity matrix. In accordance with [28]–[30], the sensor fault model can be represented by the pseudo-actuator model, without loss of generality, such as

$$\begin{aligned} \dot{x} &= Ax + E_u d + E_r \dot{z}_r + E_{fs} F_s + E_{fu} F_u \\ y &= Cx + F_u d \end{aligned} \tag{6}$$

where $F_s = \begin{bmatrix} \dot{f}_s & -f_s \end{bmatrix}^T$, $F_u = \begin{bmatrix} \dot{f}_u & -f_u \end{bmatrix}^T$, $E_{fs} = \begin{bmatrix} j_s & Aj_s \end{bmatrix}$, $E_{fu} = \begin{bmatrix} j_u & Aj_u \end{bmatrix}$, $j_{s,u}$ is the solution to $\tilde{F}_{fs,fu} = Cj_{s,u}$. Note that the derivative of the sensor fault signal is not important, and therefore it is considered another disturbances. In conclusion, the final form of the fault model of vehicle suspension is represented as

$$\begin{aligned} \dot{x} &= Ax + E_{aug} d_{aug} + E_f f \\ y &= Cx + F_{aug} d_{aug} \end{aligned} \tag{7}$$

where $E_{aug} = \begin{bmatrix} E_u & E_r & j_s & j_u \end{bmatrix}$, $E_f = \begin{bmatrix} Aj_s & Aj_u \end{bmatrix}$, $F_{aug} = \begin{bmatrix} F_d & 0 & 0 & 0 \end{bmatrix}$, $d_{aug} = \begin{bmatrix} d & \dot{z}_r & \dot{f}_s & \dot{f}_u \end{bmatrix}^T$, $f = \begin{bmatrix} -f_s & -f_u \end{bmatrix}^T$.

III. FAULT DETECTION AND ISOLATION ALGORITHM

In this section, the proposed model-based FDI algorithm is designed. Generally, the model-based FDI algorithm consists of a residual generator that generates a residual signal indicative of a fault and a residual evaluator that determines whether a fault occurs based on the residual. First, the FIO based on the quarter-car model, developed in the previous section, is designed using the eigenstructure assignment method. The FIO generates a residual signal that indicates the fault of the sprung mass accelerometer and the unsprung mass accelerometer, respectively. Next, the SVM based residual evaluator is proposed. This residual evaluator can reduce the time and effort required for traditional threshold tuning. In conclusion, the proposed FDI algorithm is implemented as shown in Fig. 2.

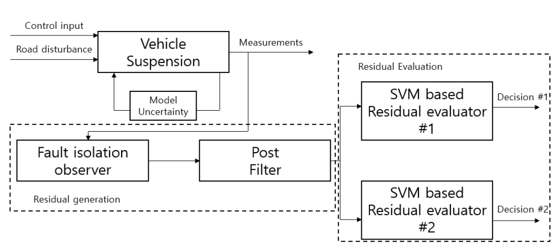

Fig. 2. Schematic description of the FDI algorithm.

A. Fault isolation observer based residual generator design

In this subsection, a fault isolation observer is designed to generate residuals for each sensor fault. The form of the fault isolation observer proposed in this paper is given as

$$\begin{aligned} \dot{\hat{x}} &= A\hat{x} - L(y - C\hat{x}) \\ r &= V(y - C\hat{x}) \end{aligned} \tag{8}$$

where $\hat{x}$ is the estimated state, L is the observer gain, r is the residual vector, and V is the post filter. Assume that the error state is defined as $e = x - \hat{x}$. The error dynamics is then given as

$$\begin{aligned} \dot{e} &= (A + LC)e + E_f f + (E_{aug} + LF_{aug})d_{aug} \\ r &= VCe + VF_{aug}d_{aug} \end{aligned} \tag{9}$$

According to (7) and (8), the transfer matrix from the fault vector f to the residual vector r is given as

$$G_{rf}(s) = VC(sI - (A + LC))^{-1}E_f \tag{10}$$

The purpose of the fault isolation observer is to diagonalize the transfer matrix. Therefore, if one fault occurs, only one residual signals is affected. In order to design such a fault isolation observer, the eigenstructure assignment method is used in this paper. Using the eigenstructure assignment method, the observer gain L and the post filter V are obtained by the following theorem [31], [32].

Theorem 1: If a system (7) fulfilled assumption described below,

- Assumption 1: (A, C) is observable
- Assumption 2: $rank(C)$ is equal to the number of measurements
- Assumption 3: $rank(P = CE_f)$ is equal to the number of faults
- Assumption 4: The system $(A, E_f, C, 0)$ is minimum phase

the observer gain L and post filter V are then given as

$$L = (E_f\Lambda - AE_f)(P)^{\dagger} + R(I - PP^{\dagger}) \tag{11}$$

$$V = MP^{\dagger} + S(I - PP^{\dagger}) \tag{12}$$

where $\Lambda = diag(\lambda_1, \lambda_2)$, $\lambda_i < 0$, $M = diag(m_1, m_2)$ and $P\dagger = (P^TP)^{-1}P^T$ is the Moore-Penrose pseudoinverse of matrix P. In addition, R and S are arbitrary matrices.
As a result, if there exist L and V, then the transfer matrix G_{rf} is given as

$$G_{rf}(s) = \begin{bmatrix} g_s & 0 \\ 0 & g_u \end{bmatrix} \tag{13}$$

where $g_s = \frac{m_1}{s-\lambda_1}$ and $g_u = \frac{m_2}{s-\lambda_2}$.
According to (7), the number of faults and the number of measurements are equal. Thus, the matrix P is square and invertible, and therefore $(I - PP^{\dagger})$ is a zero matrix. This means that L and V are uniquely determined when Λ and M are given. It is noteworthy that since the fault isolation observer does not satisfy perfect fault isolation with an unknown input decoupling (PFIUID) condition ($rank \begin{bmatrix} G_{rd} & G_{rf} \end{bmatrix} = rank(G_{rd}) + rank(G_{rf})$), the observer cannot decouple the unknown disturbance E_{aug}. In conclusion, the problem of designing robust fault isolation observers is the same as determining Λ and M to make the observer robust against unknown disturbances. At the same time, the fault sensitivity performance should be considered. This paper uses the H_- and H_∞ performance indexes [33]–[36] to evaluate the performance of FIO. These performance indexes are defined as

$$\|G_{rf}(s)\|_- = \inf_{\omega \in [\omega_1, \omega_2]} \sigma_-(G_{rf}(j\omega)) \tag{14}$$

$$\|G_{rd}(s)\|_\infty = \sup_{\omega \in [\omega_1, \omega_2]} \sigma^-(G_{rd}(j\omega)) \tag{15}$$

where σ^- is the largest singular value of G_{rd}, σ_- is the smallest singular value of G_{rf}, and ω_1 and ω_2 are the minimum and maximum frequencies of the frequency range of interest. Note that $\|G_{rf}(s)\|_-$ denotes the minimum influence of the fault on the residual signal over the frequency range of interest. Similarly, $\|G_{rd}(s)\|_\infty$ denotes the maximum influence of the disturbance on the residual signal over the frequency range of interest. Generally, these two performance indexes have a trade-off relationship. Therefore, it is impossible to design an FDI algorithm that is both robust to disturbances and sensitive to faults. However, if the performance of the FDI algorithm is defined as H_-/H_∞, then an optimized FDI algorithm using this performance index can be designed. In this paper, the eigenstructure Λ is set considering the performance index in the frequency range from 0.2hz to 20hz where the driving quality is mainly evaluated. Fig. 3 and Fig. 4 show the performance indices of residual 1 and residual 2 obtained by theorem 1 and the quarter-car model properties in Table I. Based on these results, the eigenstructure Λ is defined as $diag(-1, -0.35)$ and M is defined as an identity matrix. As a result, the observer gain L and the post filter V of the observer based residual generator are as follows.

$$L = \begin{bmatrix} 0.0920 & 0.0027 \\ -0.5368 & 0.1096 \\ 0.3697 & 0.1065 \\ 0.1289 & -0.9628 \end{bmatrix} \tag{16}$$

$$V = \begin{bmatrix} -0.4632 & -0.1096 \\ -0.3682 & -0.1062 \end{bmatrix} \tag{17}$$

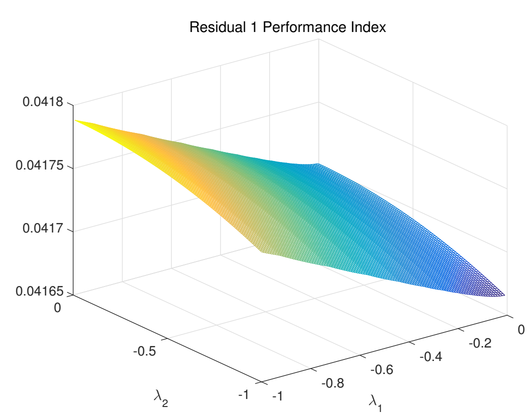

Fig. 3. Performance index for residual 1.

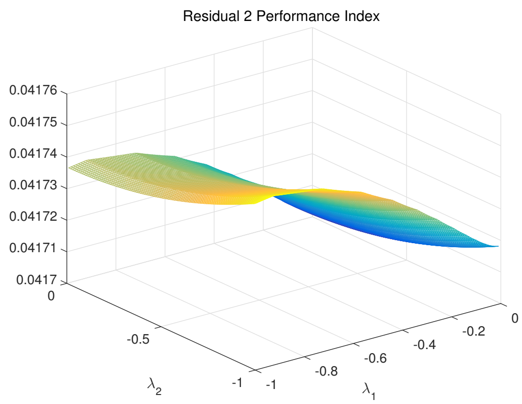

Fig. 4. Performance index for residual 2.

B. Residual evaluation based on SVM

Ideally, if there are no faults, the residuals from the residual generator have to be zero. However, in the real world there are always unexpected model uncertainties, unknown inputs and noise. Therefore, the residual evaluator is necessary to ensure the robustness of the fault diagnosis algorithm. Most residual evaluations are performed using fixed thresholds. However, it takes a lot of effort to determine the thresholds for optimal performance. Moreover, fixed thresholds are vulnerable to model uncertainty and disturbance that are not considered. Although an adaptive threshold concept was proposed in some previous studies, designing adaptive thresholds is still a difficult task.
Therefore, this paper proposes a SVM based residual evaluation method. SVM is a kind of machine-learning algorithm optimized for classification and requiring a small data set. Therefore, it can be concluded that SVM is an appropriate method to evaluate the residual signal. Fig. 5 shows the concept of the SVM classifier. In this figure, the positive class (blue-o) and negative class (red-x) are separated by the decision boundary. The decision boundary can be described as a hyperplane, as follows:

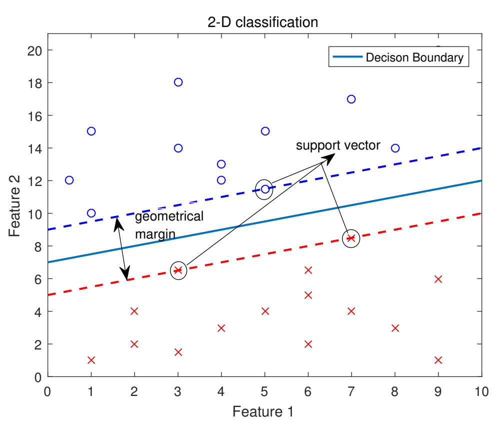

Fig. 5. Basic concept of support vector machine.

$$f(\mathbf{x}) = \mathbf{w}^T \cdot \mathbf{x} + b = 0 \tag{18}$$

where $\mathbf{x}$ is a features of the data, $\mathbf{w}$ is the normal vector of the hyperplane, and b is the bias factor. To classify the dataset, the labels are assigned as $y_i = 1$ for a positive class and $y_i = -1$ for a negative class, where $i = 1, 2, ..., N$, N is the number of data sets, and the hyperplane must satisfy the following constraints:

$$\begin{aligned} f(\mathbf{x}_i) &= 1 \quad \text{if} \quad y_i = 1 \\ f(\mathbf{x}_i) &= -1 \quad \text{if} \quad y_i = -1 \end{aligned} \tag{19}$$

These two constraints can be presented in a simple equation as follows:

$$y_i(\mathbf{w}^T \cdot \mathbf{x}_i + b) \geq 1 \tag{20}$$

SVM is based on the structural risk minimization principle [25]. Therefore, it is necessary to solve the optimization problem in order to find the optimal decision boundary having the maximum classification margin. The classification margin is described as the distance from the nearest dataset to the hyperplane. In the SVM theory, the nearest dataset is named a support vector. The distance r between the support vector $\mathbf{x}$ and a point on the hyperplane $\mathbf{x_h}$ is expressed as shown below.

$$\mathbf{x} = \mathbf{x}_h + r\frac{\mathbf{w}}{\|\mathbf{w}\|} \tag{21}$$

$$f(\mathbf{x}_h) = 0 \tag{22}$$

By substituting (21) and (22) into (18), the following equation is obtained:

$$f(\mathbf{x}) = \mathbf{w}^T \cdot \mathbf{x} + b = \mathbf{w}^T \cdot \left(\mathbf{x}_h + r\frac{\mathbf{w}}{\|\mathbf{w}\|} \right) + b = r\|\mathbf{w}\| \tag{23}$$

Therefore,

$$r = \frac{f(\mathbf{x})}{\|\mathbf{w}\|} \tag{24}$$

As a result, the problem of maximizing the distance r can be expressed as follows.

$$\min_{\mathbf{w},b} \frac{1}{2}\|\mathbf{w}\|^2 \,\text{subject to}\, (\mathbf{w}^\mathbf{T} \cdot \mathbf{x} + b)y \geq 1 \tag{25}$$

To apply this theory in the real world, the noise and reliability of the data set should be considered. Therefore, in most SVM applications, a slack variable is assigned to handle errors in the data set. Consequently, the optimal decision boundary can be obtained by the following problem:

$$\begin{aligned} &\min_{\mathbf{w},b} \tfrac{1}{2}\|\mathbf{w}\|^2 + C\sum_{i=1}^{N}\xi_i \\ &\text{subject to} \begin{cases} (w \cdot x_i + b)y_i \geq 1 - \xi_i \\ \xi_i \geq 0 \end{cases} \end{aligned} \tag{26}$$

In addition, using the mathematical techniques such as the Lagrangian multiplier and the Karush-Kuhn-Tucker (KKT) condition [37], the optimization problem (26) can be converted as follows [24]:

$$\begin{aligned} \min L(w, b, \xi, \alpha) &= \frac{1}{2}\|\mathbf{w}\|^2 \\ &+ C\sum_{i=1}^{N}\xi_i - \alpha_i y_i(\mathbf{w}^T \cdot \mathbf{x} + b - 1 + \xi_i) \end{aligned} \tag{27}$$

Using the KKT condition to eliminate the duality gap,

$$\frac{\partial L}{\partial \mathbf{w}} = 0,\ \frac{\partial L}{\partial b} = 0 \tag{28}$$

$$\alpha_i \geq 0 \text{ for } \forall i \tag{29}$$

$$\alpha_i((\mathbf{w}^T \cdot \mathbf{x}_j + b)y_j - 1) = 0 \text{ for } \forall i \tag{30}$$

Therefore,

$$\mathbf{w} = \sum_{i=1}^{N} \alpha_i y_i \mathbf{x}_i,\ \sum_{i=1}^{N} \alpha_i y_i = 0 \tag{31}$$

Consequently, using (31) and (27), the quadratic optimization problem is obtained by

$$\begin{aligned} &\max L(\alpha) = \sum_{i=1}^{N} \alpha_i - \tfrac{1}{2} \sum_{i=1}^{N} \sum_{j=1}^{N} \alpha_i \alpha_j y_i y_j {\mathbf{x}_i}^T \mathbf{x}_j \\ &\text{subject to } \alpha_i \geq 0,\ \sum_{i=1}^{N} \alpha_i y_i = 0 \end{aligned} \tag{32}$$

The above optimization problem can only be applied to classification problems with a linear decision boundary. However, with kernel functions [25], a nonlinear decision boundary can be designed while maintaining this concept. Based on the kernel function, the optimization problem (32) can be rewritten as

$$\begin{aligned} &\max L(\alpha) = \sum_{i=1}^{N} \alpha_i - \tfrac{1}{2} \sum_{i=1}^{N} \sum_{j=1}^{N} \alpha_i \alpha_j y_i y_j K(\mathbf{x}_i, \mathbf{x}_j) \\ &\text{subject to } \alpha_i \geq 0,\ \sum_{i=1}^{N} \alpha_i y_i = 0 \end{aligned} \tag{33}$$

In this paper, a residual evaluation is conducted by SVM using different kernel functions such as linear, polynomial, Gaussian RBF. In order to reduce the effect of sensor noise, preprocessing such as low pass filtering is performed. The feature for SVM learning consists of the mean and variance of a scaled residual, which is commonly used in previous machine learning applications. In the following section, the residual evaluation performance of SVM is verified using well-known performance measures for machine learning.

IV. Experimental validation

In this section, an experimental validation is conducted using a quarter-car test rig. This section is organized as follows. First, the performance of FIO proposed in this paper is verified using experimental results. The experimental road input consists of sine wave, sine sweep and rectangular wave modes. Next, SVM learning is conducted using the sensor signal and the residual signals obtained with the proposed FIO. Finally, the performance of the residual evaluator is measured using well-known machine learning performance indexes.

A. Experimental set-up

To verify the proposed FDI algorithm, a quarter-car test rig is used, which is used widely to develop suspension control systems in many previous studies. In this study, the front suspension of a Hyundai Genesis Coupe (midsize coupe) is used. In order to obtain actual states such as the suspension displacement and relative velocity, a linear variable differential transformer (LVDT) (SLS130) is attached to the suspension. In addition, to ensure practicality of the proposed algorithm, a MANDO accelerometer, which is actually used in the Hyundai Genesis Coupe, is attached to a sprung mass and an unsprung mass. The measuring range of the sprung mass accelerometer is ±2g and the measuring range of the unsprung mass accelerometer is ±50g.

TABLE II
Experimental scenarios

Case	Road input	Frequency range of interest
1	Sine wave	Low
2	Sine sweep	Mid range
3	Rectangular wave	High

The experimental validation is performed under three road surfaces. First, a low frequency sine wave road test with an elevation of +0.02 meter to -0.02 meter was performed to evaluate the performance of the proposed FDI algorithm in a low frequency range. Nest, a sine sweep road test with an elevation of -0.018 meter to +0.018 meter was performed. Finally, a rectangular wave road test with an elevation of -0.02 meter to +0.02 meter was performed to evaluate the performance of the proposed FDI algorithm in a high frequency range. The sensor faults are implemented with a data acquisition unit consisting of Micro AutoBox, Matlab&Simulink and Lenovo Thinkpad. Fig. 6 shows the experimental equipment and Table II summarize the experimental scenarios to verify the fault diagnosis performance. The physical characteristics of the quarter-car test rig are listed in Table I.

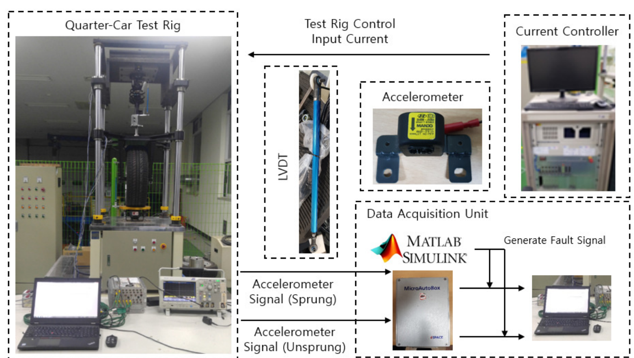

Fig. 6. Overall experimental scheme.

B. Experimental results

1) Case 1 - Sine wave test: Fig. 7 shows the results of the sine wave test. In this test scenario, a +0.5m/s^2 fault signal is added to the sprung mass accelerometer at four seconds and this fault signal is also added to the unsprung mass accelerometer at 17 seconds. To emphasize the performance of the model-based fault diagnosis algorithms, this paper did not consider fault signals such as signal loss that can be detected by traditional limit checking methods. According to the test results, it is verified that residual 1 responds only to a fault in the sprung mass accelerometer. Likewise, the other residual responds only to a fault of the unsprung mass accelerometer.

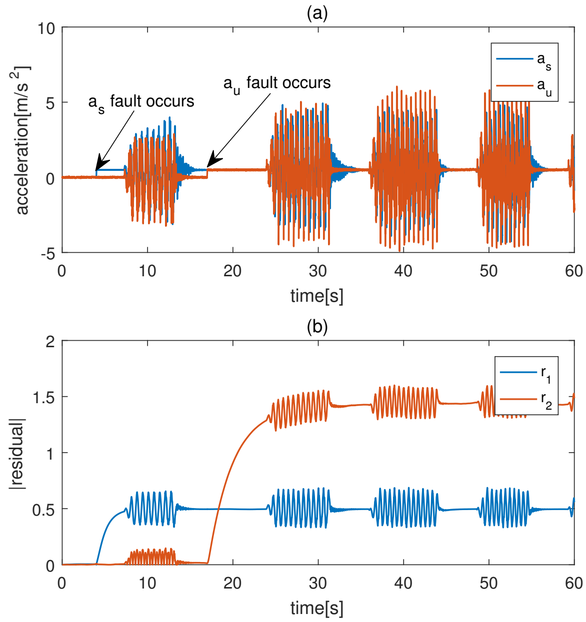

Fig. 7. Sine wave test results for fault detection and isolation: (a) Raw sensor signal of sprung mass accelerometer (a_s) and unsprung mass accelerometer (a_u) (b) Absolute value of residual 1 (r_1) and residual 2 (r_2).

This phenomenon appears prominently between four and 17 seconds in Fig. 7. In accordance with this experimental results, it is confirmed that the observer gain (16) and the post filter (17) obtained using theorem 1 make the fault transfer matrix a diagonal matrix, as in (13). The experimental results show that there is a slight response delay in the residual signal since the signal preprocessing process such as low pass filtering.

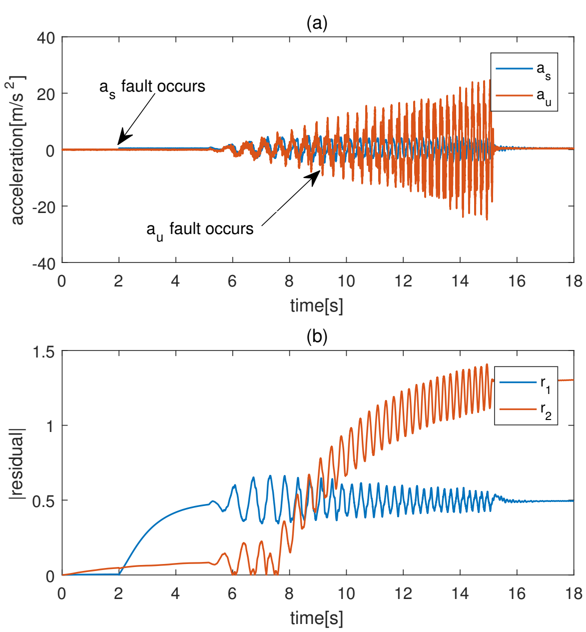

Fig. 8. Sine sweep test results for fault detection and isolation: (a) Raw sensor signal of sprung mass accelerometer (a_s) and unsprung mass accelerometer (a_u) (b) Absolute value of residual 1 (r_1) and residual 2 (r_2).

2) Case 2 - Sine sweep test: Fig. 8 shows the results of the sine sweep test. In this test scenario, a +0.5m/s^2 fault signal is added to the sprung mass accelerometer at two seconds and this fault signal is also added to the unsprung mass accelerometer at seven seconds. Unlike the sine wave test in case 1, the signal range of the unsprung mass accelerometer is as large as $\pm$30m/s^2. The experimental results show that residual 1 responds only to a fault of the sprung mass accelerometer and residual 2 responds only to a fault of the unsprung mass accelerometer. Fig. 8 shows that the residual 2 tends to increase finely between 0 and 7 seconds. This is due to the initial sensor bias in the unsprung mass accelerometer. This sensor bias is converted to a bias of residual 2.

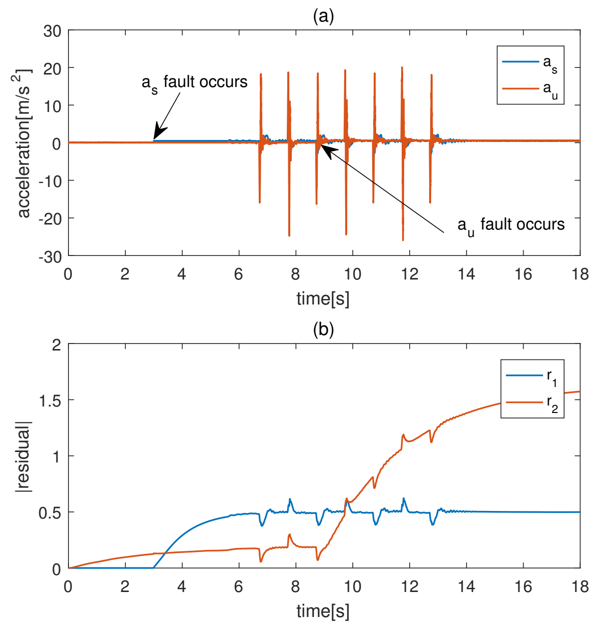

Fig. 9. Rectangular wave test results for fault detection and isolation: (a) Raw sensor signal of sprung mass accelerometer (a_s) and unsprung mass accelerometer (a_u) (b) Absolute value of residual 1 (r_1) and residual 2 (r_2).

3) Case 3 - Rectangular wave test: Fig. 9 shows the results of the rectangular wave test. In this test scenario, a +0.5m/s^2 fault signal is added to the sprung mass accelerometer at three seconds and this fault signal is also added to the unsprung mass accelerometer at nine seconds. In accordance with the experimental results, it is verified that FIO has robust performance against high frequency road input. As in case 2, residual 2 showed a slight increase between 0 and 9 seconds due to the initial sensor bias. This experimental results show that the disturbance effect on the residual is attenuated as compared with the low frequency road surface test such as case 1. This is because the fault transfer matrix (13) is in the form of a first order low pass filter. In addition, the preprocessing of the residual signal also reduces the effect of high frequency disturbance.

C. Residual evaluation result

In this paper, the authors propose to evaluate the residual signal obtained by FIO using the SVM classifier. This section presents and discusses the residual evaluation results obtained using various SVM classifiers with different kernel functions. The data set for learning the SVM classifier is obtained by various experiments using quarter-car test equipment. Sensor signals and residual signals obtained from various experiments were classified as faulty data and healthy data respectively and used for learning. In this paper, 189003 data sets were used and the standard deviation and mean value of each data set were chosen as the features to be used for SVM learning.

In order to verify the performance of the SVM based residual evaluation, five-cross validation and the $F_{0.5}$-Measure are used. Generally, the fault diagnosis algorithm used in vehicle systems should be designed to minimize false alarms where faults are detected in the absence of actual faults. Therefore, it is reasonable to use the $F_{0.5}$-Measure, which emphasizes precision rather than recall, to evaluate the performance of the fault diagnosis algorithm. In this paper, various types of SVM classifiers are constructed using Matlab & Simulink quadratic programming solver.

Table III and Table IV show the classification results using SVM classifiers with various kernel functions. As presented in the tables, the SVM based residual evaluator achieves high accuracy. Since the initial bias is on the unsprung mass accelerometer, the classification performance for residual 2 is slightly lower than the classification performance for residual 1. Overall, the SVM classifier achieved high accuracy. In order to investigate the effect of residuals on fault decision, SVM leaning was conducted using only sensor signals with no residuals. From the results of SVM leaning without residuals, the SVM classifier accuracy is around 0.75. In conclusion, it is confirmed that residuals have a positive effect on SVM classifier learning.

TABLE III
SVM CLASSIFIER PERFORMANCE OUTCOMES FOR RESIDUAL 1

Kernel function	Kernel scale	$F_{0.5}$-Measure
Linear	-	0.997
Quadratic	-	0.997
Gaussian RBF	0.5	0.998
Gaussian RBF	2	0.999

TABLE IV
SVM CLASSIFIER PERFORMANCE OUTCOMES FOR RESIDUAL 2

Kernel function	Kernel scale	$F_{0.5}$-Measure
Linear	-	0.994
Quadratic	-	0.996
Gaussian RBF	0.5	0.996
Gaussian RBF	2	0.997

Fig. 10 and Fig. 11 show confusion matrices of the SVM classifiers for residual evaluation. These figures show that as the nonlinearity of the decision boundary increases, false positive error tends to increase. Generally, a nonlinear decision boundary exhibits higher accuracy than linear decision boundaries, but over fitting can occur. In conclusion, the false positive error in Fig. 10 and Fig. 11 is due to overfitting. As mentioned above, the fault diagnosis algorithm used in vehicle systems should be designed to minimize false positive errors. In accordance with Fig. 10, neither the linear nor quadratic SVM classifier exhibits false positive error.

Fig. 12 and Fig. 13 show the residual evaluation results of the sine wave and sine sweep experiments. Note that these experiments are conducted in order to verify the performance of the SVM based residual evaluator. Therefore, the data sets of these experiments are different from the learning data. In these experiments, a $+0.5\text{m/s}^2$ fault signal is added to the sprung mass accelerometer at five seconds and this fault signal is also added to the unsprung mass accelerometer at 10 seconds. According to the experimental results, false alarms do not occur and error cases consist only of false negative error. This false negative error is caused by the residual response delay due to the preprocessing such as low pass filtering. In conclusion, the SVM based residual evaluator presents reasonable performance for a vehicle suspension sensor system.

Fig. 10. Confusion matrix of SVM classifiers for evaluation residual 1: (a) Linear SVM (b) Quadratic SVM (c) Gaussian RBF SVM with Kernel scale = 2 (d) Gaussian RBF SVM with Kernel scale = 0.5.

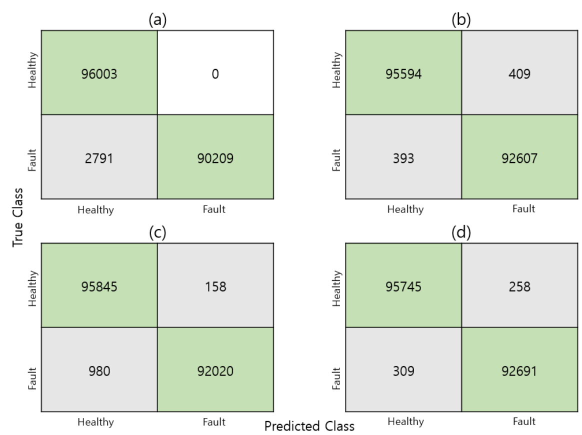

Fig. 11. Confusion matrix of SVM classifiers for evaluation residual 2: (a) Linear SVM (b) Quadratic SVM (c) Gaussian RBF SVM with Kernel scale = 2 (d) Gaussian RBF SVM with Kernel scale = 0.5.

Fig. 14 and Fig. 15 show the residual evaluation results for signal loss fault. According to Fig. 14, the sprung mass accelerometer signal is lost at seven seconds and this signal is recovered at 15 seconds. In this experimental scenario, the unsprung mass accelerometer is fault free but residual 2 is

not zero due to the sensor bias. However, the fault index F_u is zero during the experimental scenario. This experimental result show that the SVM-based residual evaluation algorithm makes accurate decision despite the presence of unconsidered sensor bias. Likewise, according to Fig. 15, the unsprung mass accelerometer signal is lost at seven seconds. In this experimental scenario, the sprung mass accelerometer is fault free and the fault index F_s is zero during the experimental scenario same as Fig. 14.
Fig. 16 and Fig. 17 show the residual evaluation results for random noise fault. According to Fig. 16, the sprung mass accelerometer signal is contaminated with random noise at 12 seconds. Likewise, according to Fig. 17, the unsprung mass accelerometer signal is contaminated with random noise at 12 seconds. As a results of these experiments, it is conclude that the proposed fault diagnosis algorithm has robust performance for random noise fault. Consequently, the experimental results show that the proposed residual evaluation method has reasonable performance against unconsidered sensor bias and untrained type of fault.
It is note worthy that the SVM classifier used in this paper does not learn about signal loss fault. In general, machine learning algorithms are vulnerable to untrained data types. However, the proposed SVM classifier uses the residuals obtained by the model-based fault diagnosis technique in the learning procedure. This can complement the weaknesses of traditional machine learning algorithms and show reasonable performance against untrained type of fault.

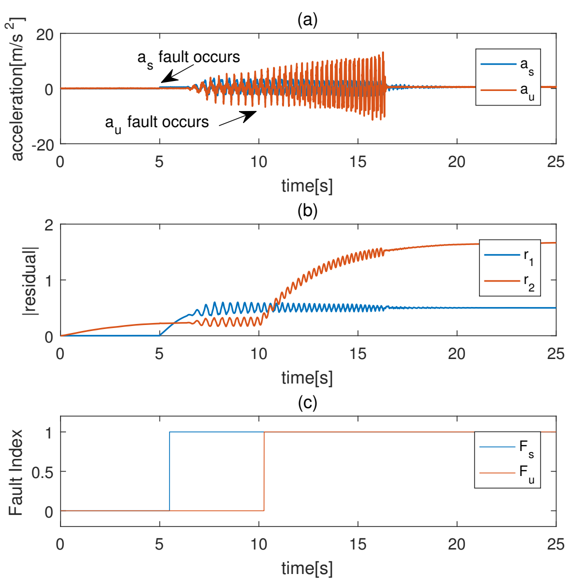

Fig. 12. Experimental result for sine sweep test: (a) Raw sensor signal of sprung mass accelerometer (a_s) and unsprung mass accelerometer (a_u) (b) Absolute value of residual 1 (r_1) and residual 2 (r_2) (c) Fault indicator for sprung mass accelerometer (F_s) and unsprung mass accelerometer (F_u).

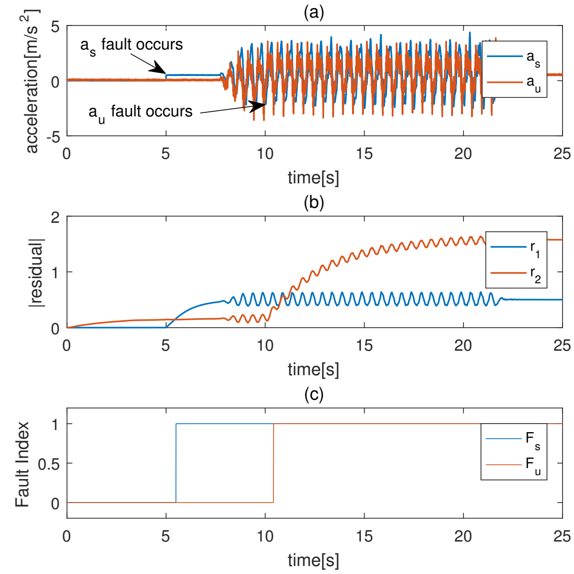

Fig. 13. Experimental result for sine wave test: (a) Raw sensor signal of sprung mass accelerometer (a_s) and unsprung mass accelerometer (a_u) (b) Absolute value of residual 1 (r_1) and residual 2 (r_2) (c) Fault indicator for sprung mass accelerometer (F_s) and unsprung mass accelerometer (F_u).

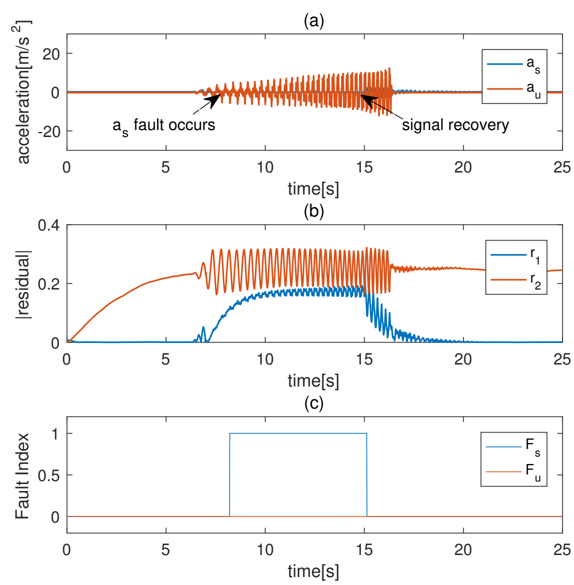

Fig. 14. Experimental result for signal loss(sine sweep test): (a) Raw sensor signal of sprung mass accelerometer (a_s) and unsprung mass accelerometer (a_u) (b) Absolute value of residual 1 (r_1) and residual 2 (r_2) (c) Fault indicator for sprung mass accelerometer (F_s) and unsprung mass accelerometer (F_u).

V. Conclusion

In this paper, a fault diagnosis algorithm for a vehicle suspension sensor is proposed. The proposed fault diagnosis algorithm consists of FIO that generates a residual signal and a SVM based residual evaluator. Using the eigenstructure assignment method and H_-/H_∞ performance index, FIO, which is both robust against unknown disturbance and sensitive to sensor fault, is designed. In addition, using the residuals generated by FIO for SVM training, this paper combines model-based fault diagnosis with machine learning based fault

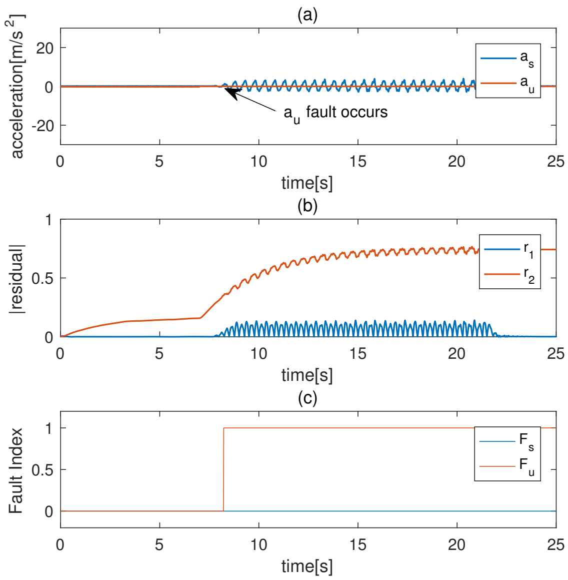

Fig. 15. Experimental result for signal loss(sine wave test): (a) Raw sensor signal of sprung mass accelerometer (a_s) and unsprung mass accelerometer (a_u) (b) Absolute value of residual 1 (r_1) and residual 2 (r_2) (c) Fault indicator for sprung mass accelerometer (F_s) and unsprung mass accelerometer (F_u).

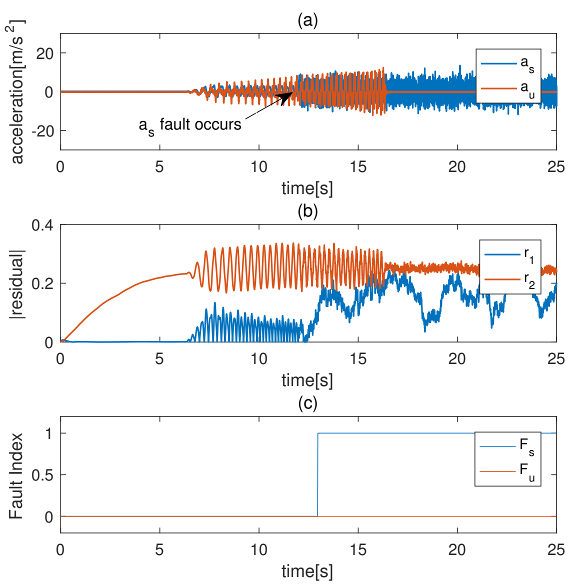

Fig. 16. Experimental result for random noise fault(sine sweep test): (a) Raw sensor signal of sprung mass accelerometer (a_s) and unsprung mass accelerometer (a_u) (b) Absolute value of residual 1 (r_1) and residual 2 (r_2) (c) Fault indicator for sprung mass accelerometer (F_s) and unsprung mass accelerometer (F_u).

diagnosis. This paper also validates the performance of FIO and SVM based residual evaluator using a quarter-car test rig and commercial sensors. From the results, it is confirmed that an isolated residual signal is generated by FIO regardless of an unknown disturbance. Furthermore, it is verified that the SVM based residual evaluator has high accuracy for various

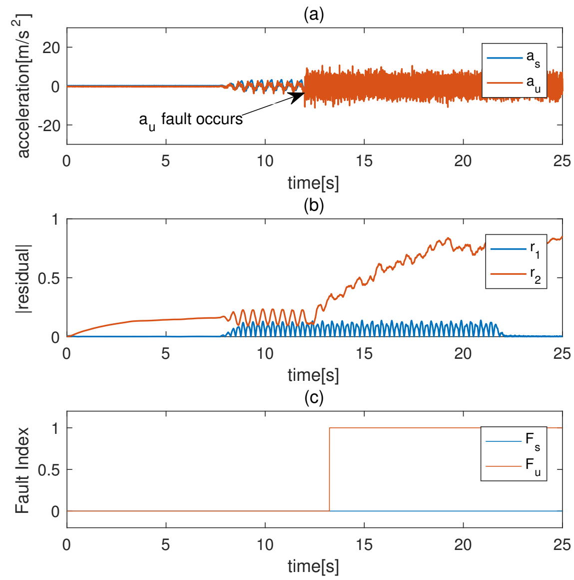

Fig. 17. Experimental result for random noise fault(sine wave test): (a) Raw sensor signal of sprung mass accelerometer (a_s) and unsprung mass accelerometer (a_u) (b) Absolute value of residual 1 (r_1) and residual 2 (r_2) (c) Fault indicator for sprung mass accelerometer (F_s) and unsprung mass accelerometer (F_u).

road inputs and robust against untrained type of fault.
This paper provides the following contributions. First, the proposed fault diagnosis algorithm considers a practical suspension sensor system. A commercial accelerometer used in practical fields is used to verify the performance of the fault diagnosis algorithm. In addition, using a quarter-car test rig and the commercial accelerometer, the practicality of the proposed fault diagnosis algorithm is confirmed. Next, the proposed fault diagnosis algorithm can be used in any kind of semi-active suspension system. Since the bilinear term coupled with control input and unknown system state is converted to modeling uncertainty, it is possible to adopt the proposed fault diagnosis algorithm when the damping coefficient range of the vehicle suspension system is known. Finally, this paper verified that the SVM based residual evaluator can replace the heuristically tuned residual threshold. It thus becomes possible to reduce the effort required to design fault diagnosis algorithms. In conclusion, the proposed fault diagnosis algorithm can be used to detect sensor faults in vehicle suspension.

Acknowledgment

This work was supported by the Technology Innovation Program (or Industrial Strategic Technology Development Program (10084619, Development of Vehicle Shock Absorber (Damper) and Engine Mount Using MR Fluid with Yield Strength of 60kPa) funded By the Ministry of Trade, Industry & Energy (MOTIE, Korea); the BK21+ program through the NRF funded by the Ministry of Education of Korea; the National Research Foundation of Korea(NRF) grant funded by the Korea government(MSIP) (No. 2017R1A2B4004116)

References

[1] J. Swevers, C. Lauwerys, B. Vandersmissen, M. Maes, K. Reybrouck, and P. Sas, "A model-free control structure for the on-line tuning of the semi-active suspension of a passenger car," *Mechanical Systems and Signal Processing*, vol. 21, no. 3, pp. 1422–1436, 2007.

[2] S. M. Savaresi and C. Spelta, "A single-sensor control strategy for semi-active suspensions," *IEEE Transactions on control systems Technology*, vol. 17, no. 1, pp. 143–152, 2009.

[3] H.-S. Roh and Y. Park, "Preview control of active vehicle suspensions based on a state and input estimator," SAE Technical Paper, Tech. Rep., 1998.

[4] D. Karnopp, M. J. Crosby, and R. Harwood, "Vibration control using semi-active force generators," *Journal of engineering for industry*, vol. 96, no. 2, pp. 619–626, 1974.

[5] R. Darus and Y. M. Sam, "Modeling and control active suspension system for a full car model," in *Signal Processing & Its Applications, 2009. CSPA 2009. 5th International Colloquium on*. IEEE, 2009, pp. 13–18.

[6] H.-S. Roh and Y. Park, "Observer-based wheelbase preview control of active vehicle suspensions," *KSME International Journal*, vol. 12, no. 5, pp. 782–791, 1998.

[7] O. Lindgärde, "Kalman filtering in semi-active suspension control," in *Proc. of 15th IFAC World Congress*, 2002, pp. 1539–1544.

[8] R. K. Dixit and G. D. Buckner, "Sliding mode observation and control for semiactive vehicle suspensions," *Vehicle System Dynamics*, vol. 43, no. 2, pp. 83–105, 2005.

[9] S. M. Savaresi, E. Silani, and S. Bittanti, "Acceleration-driven-damper (add): An optimal control algorithm for comfort-oriented semiactive suspensions," *Journal of dynamic systems, measurement, and control*, vol. 127, no. 2, pp. 218–229, 2005.

[10] S. M. Savaresi and C. Spelta, "Mixed sky-hook and add: Approaching the filtering limits of a semi-active suspension," *Journal of dynamic systems, measurement, and control*, vol. 129, no. 4, pp. 382–392, 2007.

[11] Z. Gao, C. Cecati, and S. X. Ding, "A survey of fault diagnosis and fault-tolerant techniquespart i: Fault diagnosis with model-based and signal-based approaches," *IEEE Transactions on Industrial Electronics*, vol. 62, no. 6, pp. 3757–3767, 2015.

[12] S. X. Ding, *Model-based fault diagnosis techniques: design schemes, algorithms, and tools*. Springer Science & Business Media, 2008.

[13] Y. Wu, B. Jiang, and N. Lu, "A descriptor system approach for estimation of incipient faults with application to high-speed railway traction devices," *IEEE Transactions on Systems, Man, and Cybernetics: Systems*, 2017.

[14] Y. Wu, B. Jiang, and Y. Wang, "Incipient winding fault detection and diagnosis for squirrel-cage induction motors equipped on crh trains," *ISA transactions*, 2019.

[15] Z. Mao, Y. Zhan, G. Tao, B. Jiang, and X.-G. Yan, "Sensor fault detection for rail vehicle suspension systems with disturbances and stochastic noises," *IEEE Transactions on Vehicular Technology*, vol. 66, no. 6, pp. 4691–4705, 2016.

[16] S. Yan, W. Sun, F. He, and J. Yao, "Adaptive fault detection and isolation for active suspension systems with model uncertainties," *IEEE Transactions on Reliability*, vol. 68, no. 3, pp. 927–937, 2018.

[17] A. Chamseddine and H. Noura, "Control and sensor fault tolerance of vehicle active suspension," *IEEE Transactions on Control Systems Technology*, vol. 16, no. 3, pp. 416–433, 2008.

[18] W. Kim, J. Lee, S. Yoon, and D. Kim, "Development of mando's new continuously controlled semi-active suspension system," SAE Technical Paper, Tech. Rep., 2005.

[19] M. Börner, R. Isermann, and M. Schmitt, "A sensor and process fault detection system for vehicle suspension systems," SAE Technical Paper, Tech. Rep., 2002.

[20] S. Varrier, R. Morales-Menendez, J. D.-J. Lozoya-Santos, D. Hernandez, J. M. Molina, and D. Koenig, "Fault detection in automotive semi-active suspension: Experimental results," SAE Technical Paper, Tech. Rep., 2013.

[21] J. Kim and H. Lee, "Sensor fault detection and isolation algorithm for a continuous damping control system," *Proceedings of the Institution of Mechanical Engineers, Part D: Journal of Automobile Engineering*, vol. 225, no. 10, pp. 1347–1364, 2011.

[22] K. Yi, "Design of disturbance decoupled bilinear observers," *KSME Journal*, vol. 9, no. 3, pp. 344–350, 1995.

[23] L. Wang, *Support vector machines: theory and applications*. Springer Science & Business Media, 2005, vol. 177.

[24] J. Liang and R. Du, "Model-based fault detection and diagnosis of hvac systems using support vector machine method," *International Journal of refrigeration*, vol. 30, no. 6, pp. 1104–1114, 2007.

[25] A. Widodo and B.-S. Yang, "Support vector machine in machine condition monitoring and fault diagnosis," *Mechanical systems and signal processing*, vol. 21, no. 6, pp. 2560–2574, 2007.

[26] Z. Gao, C. Cecati, and S. Ding, "A survey of fault diagnosis and fault-tolerant techniquespart ii: Fault diagnosis with knowledge-based and hybrid/active-based approaches," *IEEE Trans. Ind. Electron*, vol. 62, pp. 3768–3774, 2015.

[27] M. Zasadzinski, E. Magarotto, H. Rafaralahy, and H. S. Ali, "Residual generator design for singular bilinear systems subjected to unmeasurable disturbances: an lmi approach," *Automatica*, vol. 39, no. 4, pp. 703–713, 2003.

[28] W. H. Chung and J. L. Speyer, "A game theoretic fault detection filter," *IEEE Transactions on Automatic Control*, vol. 43, no. 2, pp. 143–161, 1998.

[29] X.-G. Yan and C. Edwards, "Sensor fault detection and isolation for nonlinear systems based on a sliding mode observer," *International Journal of Adaptive Control and Signal Processing*, vol. 21, no. 8-9, pp. 657–673, 2007.

[30] S. Armeni, A. Casavola, and E. Mosca, "A robust fault detection and isolation filter design under sensitivity constraint: An lmi approach," *International Journal of Robust and Nonlinear Control: IFAC-Affiliated Journal*, vol. 18, no. 15, pp. 1493–1506, 2008.

[31] Z. Li and I. M. Jaimoukha, "Observer-based fault detection and isolation filter design for linear time-invariant systems," *International Journal of Control*, vol. 82, no. 1, pp. 171–182, 2009.

[32] A. Wahrburg and J. Adamy, "Parametric design of robust fault isolation observers for linear non-square systems," *Systems & Control Letters*, vol. 62, no. 5, pp. 420–429, 2013.

[33] W. Li, Z. Zhu, G. Zhou, and G. Chen, "Optimal h i/h fault-detection filter design for uncertain linear time-invariant systems: an iterative linear matrix inequality approach," *IET Control Theory & Applications*, vol. 7, no. 8, pp. 1160–1167, 2013.

[34] J. Liu, J. L. Wang, and G.-H. Yang, "An lmi approach to minimum sensitivity analysis with application to fault detection," *Automatica*, vol. 41, no. 11, pp. 1995–2004, 2005.

[35] M. L. Rank and H. Niemann, "Norm based design of fault detectors," *International Journal of control*, vol. 72, no. 9, pp. 773–783, 1999.

[36] J. L. Wang, G.-H. Yang, and J. Liu, "An lmi approach to h-index and mixed h-/h fault detection observer design," *Automatica*, vol. 43, no. 9, pp. 1656–1665, 2007.

[37] N. Cristianini, J. Shawe-Taylor *et al.*, *An introduction to support vector machines and other kernel-based learning methods*. Cambridge university press, 2000.

Kicheol Jeong received his B.S. degree in Mechanical Engineering from Hanyang University, Busan, South Korea, and M.S. in Mechanical Engineering from the Korea Advanced Institute of Science and Technology (KAIST), in 2015 and 2017, respectively. Since 2017, he is currently pursuing the Ph.D. degree in Mechanical engineering at KAIST. His research interests include vehicle dynamics and control, fault diagnosis and control theory.

Seibum B. Choi received B.S. degree in mechanical engineering from Seoul National University, Korea, M.S. degree in mechanical engineering from Korea Advanced Institute of Science and Technology (KAIST), Korea, and the Ph.D. degree in controls from the University of California, Berkeley in 1993. Since 2006, he has been with the faculty of the Mechanical Engineering department at KAIST. His research interests include fuel saving technology, vehicle dynamics and control, and application of self-energizing mechanism.

Hyungjeen Choi recieved B.S degree in Mechanical Engineering and Electronics(minor) from Dongguk University, Korea, M.S degree in Mechatronics from Gwangju Instutitue of Science and Technology, Korea, and is currently pursuining PhD degree in Mechanical Enginnering in Korea Advanced Institute of Science and Technology (KAIST), Korea. He has joined Korea Automotive Technology Insitute(KTAECH) since 2004. He is focusing on vehicle dynamics and control, active control system, advanced driver assistnace system(ADAS), autonomous vehicle control, and micro-mobility.